IEEE Access
Multidisciplinary | Rapid Review | Open Access Journal

Received April 6, 2021, accepted April 23, 2021, date of publication May 3, 2021, date of current version May 17, 2021.

*Digital Object Identifier 10.1109/ACCESS.2021.3077065*

# Neural Networks Based Shunt Hybrid Active Power Filter for Harmonic Elimination

**MUZAMMIL IQBAL[1], MUHAMMAD JAWAD[1], MUJTABA HUSSAIN JAFFERY[1], SALEEM AKHTAR[1], MUHAMMAD NADEEM RAFIQ[1], MUHAMMAD BILAL QURESHI[2], ALI R. ANSARI[3], AND RAHEEL NAWAZ[4]**

[1]Department of Electrical and Computer Engineering, CUI Lahore Campus, Lahore 54000, Pakistan
[2]Department of Electrical and Computer Engineering, CUI Abbottabad Campus, Abbottabad 22060, Pakistan
[3]Department of Mathematics and Natural Sciences, Gulf University of Science and Technology, Mishref Campus, Hawally 32093, Kuwait
[4]Department of Operations, Technology, Events and Hospitality Management, Manchester Metropolitan University, Manchester M15 6BH, U.K.

Corresponding author: Muhammad Jawad (mjawad@cuilahore.edu.pk)

This work was supported in part by the National Research Program for Universities (NRPU), Pakistan, under Project 7807, and in part by the Gulf University of Science and Technology.

**ABSTRACT** The growing use of nonlinear devices is introducing harmonics in power system networks that result in distortion of current and voltage signals causing damage to power distribution systems. Therefore, in power systems, the elimination of harmonics is of great significance. This paper presents an efficient techno-economical approach to suppress harmonics and improve the power factor in power distribution networks using Shunt Hybrid Active Power Filters (SHAPF) based on neural network algorithms like Artificial Neural Network (ANN), Adaptive Neuro-Fuzzy Inference System (ANFIS), and Recurrent Neural Network (RNN). The objective of the proposed algorithms for SHAPF is to enhance system performance by reducing Total Harmonic Distortion (THD). In our filter design approach, we tested and compared conventional pq0 theory and neural networks to detect the harmonics present in the power system. Moreover, for the regulation of DC supply to the inverter of the SHAPF, the conventional PI controller and neural networks-based controllers are used and compared. The applicability of the proposed filter is tested for three different nonlinear load cases. The simulation results show that the neural networks-based filter control techniques satisfy all international standards with minimum current THD, neutral wire current elimination, and small DC voltage fluctuations for voltage regulation current. Furthermore, the three neural network architectures are tested and compared based on accuracy and computational complexity, with RNN outperforming the rest.

**INDEX TERMS** Harmonic analysis, neural networks, power harmonic filters, power system analysis computing, total harmonic distortion.

## I. INTRODUCTION

The performance of electrical devices has been steadily improving with advancements in power electronics. However, the use of nonlinear load tends to degrade the sinusoidal electric supply. Instead of conducting in a smooth manner, the nonlinear loads draw current in short pulses and introduce harmonics in the system. This issue of harmonics is not confined to industrial users; it affects the domestic users as well. The use of uninterrupted power supplies, computers, LED light bulbs, LCDs, fans, and refrigerators are common in commercial and residential sectors. Moreover, the use of distributed resources to fulfill the energy demands affects the power transmission similar to the nonlinear loads.

The associate editor coordinating the review of this manuscript and approving it for publication was Jamshid Aghaei.

The distribution transformer in saturation becomes a source of harmonics and heats up due to the increased circulating current in the delta connection. Because of the triplen harmonics, the current contains zero sequence along with the positive sequence. Zero sequence current causes the flow of large currents through the neutral wire. The electric system suffers the unexpected operation of protective relays due to harmonic distortions. Moreover, due to harmonics, insulation of conductors is damaged, loss of mechanical parts in electric motors occurs, and interference in telecommunication lines is introduced. To limit the extent of harmonics in the power system, international standards, such as IEEE-519 and IEC-61000 have been introduced [1]. These standards suggest possible recommendations to minimize current and voltage distortions to a tolerable level.

To address this problem of harmonic contamination in the power system, researchers have presented different

techniques to suppress harmonic distortion. For example, installation of capacitor banks has been suggested as a low cost and simple solution to eliminate harmonics in the power system. However, in the case of overvoltage or undesired fuse operation, a threat appears to shorten the life of the capacitor banks through the insulation breakdown [2]. Moreover, the issue of resonance arises when the reactance offered by the capacitor bank becomes equal to the system inductive reactance at a certain time instant. Therefore, the use of capacitor banks to eliminate harmonics in voltage and current signals is not encouraged. One of the widely used solutions against harmonics in the industrial sector is the use of passive filters tuned for single frequency or a specific band of frequencies [3]. Passive filters mitigate the harmonics by providing a low resistance path to the tuned harmonic current [4]. However, due to undesired resonance present in the high voltage systems, the use of passive filters cannot guarantee desired results. Moreover, the compensation execution is fixed in case of passive filters. Active power filters are favored over passive filters because active filters eliminate the issue of resonance and mitigate the detected harmonics in the system [5]. However, the use of active filters for harmonics elimination is very costly. Therefore, an intermediate solution (between passive and active filters) known as hybrid active filter has been described as the most suitable solution for the harmonic elimination [6]. In this paper, we present the use of Shunt Hybrid Active Power Filters (SHAPF) for harmonic elimination in power distribution systems. The efficiency of the SHAPF is improved using neural network based adaptive controllers, such as Artificial Neural Network (ANN), Adaptive Neuro Fuzzy Inference System (ANFIS), and Recurrent Neural Network (RNN).

The main contributions of the paper are as follows:

- To address the problem of harmonic distortion, neural networks based SHAPF are designed and compared for an unbalanced three phase four-wire power system.
- First, a conventional SHAPF is designed for comparison and decision-making, where the voltage regulation circuit and reference current detection circuits are implemented using PI controller and instantaneous active and reactive power theory (pq0), respectively.
- The control circuit of the SHAPF is improved using three different neural network-based techniques, such as ANN, ANFIS, and RNN for three different nonlinear load cases. To the best of our knowledge, ANFIS and RNN based predictive control techniques are used for the first time in the control circuitry of the SHAPF, where RNN outperforms the rest.
- To provide a thorough review from a broad perspective, we conducted a detailed comparison between the conventional pq0 theory and PI controller-based techniques with proposed neural network based SHAPF. The results present practical need of adopting neural networks for harmonic elimination in power systems.
- To illustrate the capability of SHAPF, a thorough comparison of series and parallel resonance elimination is conducted between the conventional PPF and proposed SHAPF.

The rest of the paper is organized as follows: Section 2 presents the literature review on harmonic elimination using filters. Section 3 describes the system model using SHAPF. Section 4 describes the proposed control methodologies. Sections 5 includes the results and discussion. Section 6 concludes the articles and presents future research directions.

## II. LITERATURE REVIEW

The growing usage of nonlinear loads in residential and industrial sectors brings the problem of harmonics in the power system, which results in numerous energy losses. The efficiency and durability of the technical instruments, such as transformers and relays are affected by the presence of harmonics [7]. To improve the transmission and distribution systems, harmonic elimination is necessary. Researchers have proposed different solutions, such as Passive Power Filters (PPF) [4], [8], [9], Active Power Filters (APF) [5]–[7], [10]–[21], and Hybrid Active Power Filters (HAPF) [22]–[25], [28]. The architectural overview of research conducted in harmonic filters is graphically presented in Figure 1.

PPF is a low-cost solution to eliminate harmonics. Therefore, use of PPF to achieve a pure sinusoidal source and to reduce the energy losses has always been an attractive solution for power systems in both industrial and domestic sectors. In the design of the PPFs, various structure-based topologies have been presented but the most simple and efficient is the Single Tuned PPF (STPPF) [3]. Researchers have applied various optimization techniques to improve the response of STPPF reducing its cost and complexity. In [8], implementation of different STPPFs considering the reconfiguration of the power distribution system is presented. The author achieved a significant reduction in THD; however, complexity and system response time increased compared to the traditional technique. The STPPF should be connected in parallel to the system near the connection of the nonlinear load to achieve the better results.

Designing the parameters of filters using optimization algorithms is expected to be error free while improving system behavior. In [9], the optimal parameters for two STPPFs are determined using a multiple objective based Grasshopper Algorithm for renewable energy based on a smart grid including a nonlinear load. A comparison is made with GA based optimization algorithm to prove validity of the proposed technique. Although use of PPFs is a better economical approach towards the elimination of harmonics in a system but the approach has drawbacks: (a) The rigid nature of PPF is not suitable for variable load system, (b) Once PPF is installed in a system, it cannot easily be resized, (c) In order to eliminate more than one harmonics, more filters will be required inter-harmonics, and (e) The PPFs have resonance, this causes an enhanced impact of harmonics in the system instead of diminishing. Therefore, to avoid these drawbacks, Active Power Filters (APF) are used due to their characteristic

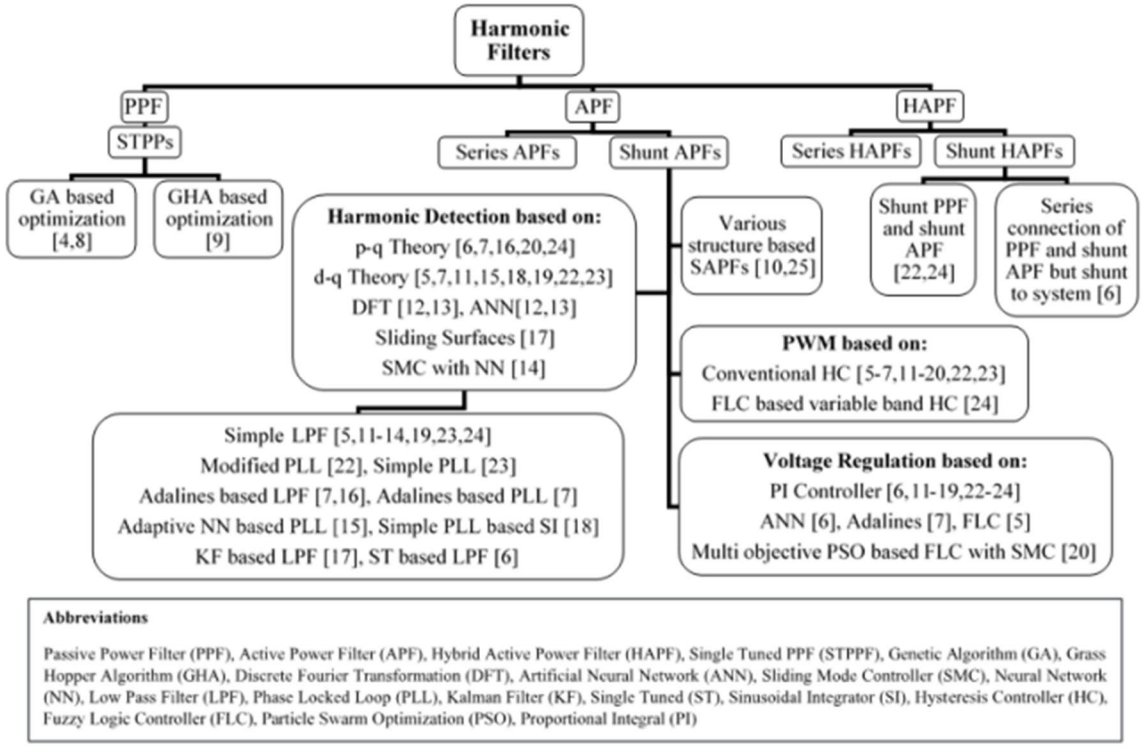


**FIGURE 1.** Taxonomy of harmonic elimination filters.

of detecting all the harmonics in the power system, improving THD, and power factor accordingly. The APF also eliminates the issue of resonance raised by PPF. Because of low copper losses in case of a parallel connection, Shunt Active Power Filters (SAPF) are found efficient among APFs [3].

For SAPFs, a lot of research has been carried out focusing the use of control techniques to ensure robustness and various structure-based topologies are introduced to reduce the structural complexity and cost of SAPFs. In [10], a comparative study and applicability of five different structure-based techniques for SAPF are analyzed using two cases differing by zero sequence current. The topology considering zero sequence current is closer to the practical situation because in actual systems the amount of current in a neutral wire is not negligible [10]. In [5], instead of using STPPF or a simple capacitor bank for the elimination of a single harmonic, SAPF is used along with the capacitor bank to improve the power factor for a variable load system. This cost-effective flexible technique is applicable to both large-scale and laboratory-scale power systems without any change.

In SAPFs, detection of harmonics, voltage regulator design and current controller design are the three main controllable parts. In the literature, we noted that various control techniques have been used for these three parts. For the detection of harmonics in a power system, there are two basic control techniques used by researchers with modifications. These basic techniques are instantaneous active and reactive power theory (p-q theory) and synchronous reference frame theory (d-q theory) [3]. For a voltage regulator, the conventional Proportional Integral (PI) control technique is proposed [6], [11]–[19], [22]–[24], and for the current controller, the hysteresis-based control is proposed [5]–[7], [11]–[20], [22], [23].

To eliminate all undesired harmonics from the system, researchers have designed SAPFs with different control techniques for the detection of harmonics present in a distorted power system. In [11], the d-q theory is used with Fourier technique for harmonic reference current generation. In [12], Artificial Neural Network (ANN) based active filter is simulated and practically verified for up to eleventh order harmonics elimination. This ANN-based more efficient APF requires only half cycle of the source current for detection of harmonics while the DFT based APF requires at least two cycles. Therefore, the ANN based is a preferable method for a system having more peak hours due to its robustness. In [13], instead of training the neural network, harmonics are determined adaptively using its fundamental principle within a half period of the fundamental considering only odd harmonics. In [14], instead of using conventional sliding mode controller only, it is employed with a sequential behavior neural network containing two hidden layers to help the former controller in determining the unknown function for the estimation of the reference harmonic current. This new composition of the controller for SAPF is better compared to a single hidden layer for the reduction of THD.

Instead of presenting a completely new technique for harmonic detection, most researchers have tried to improve the

response of p-q and d-q techniques with the use of new control methods based on Phase Locked Loop (PLL) and low pass filters. In [15], the SAPF for a three-phase balanced system is implemented using the conventional d-q theory with a novel PLL system employing an adaptive neural network technique for phase extraction. To avoid computational complexity for the estimation of the fundamental frequency, a low pass filter is utilized, and ANN is converged rapidly with a low estimation error for its weights considering only the first 13 harmonics. The technique proposed in [15] is novel; however, computationally complex, and less effective for triple and higher-order harmonics. In [16], the behavior of SAPF for a balanced supply voltage system utilizing p-q theory with the replacement of low pass filter by two Adaptive Linear Neural Networks (ADALINEs) is presented. This SAPF technique is designed for the elimination of five major odd harmonics. In [17], Kalman filter gives the average and quadrature components of voltages to the sliding surfaces that produce reference current for the elimination of harmonics. This technique gives better performance; however, there are drawbacks because of the complexity and suppositions to reduce the computational time. In [18], the PLL based sinusoidal integrator tuned for the third-order pre-filter is used to extract fundamental and quadrature components of the currents adaptively. In comparison with the traditional PLL based technique, it is found to be more robust and independent of any change in system frequency. In [7], a comparison of three various techniques for the detection of harmonics in SAPF is presented, resulting the p-q theory as the best suitable one.

To improve the performance of SAPFs, another important aspect of research is to reduce ripples in DC link voltage and steady state error of DC voltage by designing appropriate control for voltage regulator. In [19], the fuzzy controller-based technique is used instead of PI controller and synchronous reference frame-based technique is used for the detection of harmonics. In [20], multi-objective particle swarm optimization based fuzzy logic sliding mode controller is used for voltage regulation. The capacity of a harmonic filter in the case of variable speed drives in the system is typically evaluated by the measurement of harmonic current generated by these drives. In [21], the author presents the effects of active harmonic filter regarding the change in the THD for current in the system with the help of case studies, a margin factor to determine the capacity of the filter using the results of various cases is suggested.

Despite the advantages of APFs in the power distribution systems, electromagnetic interferences might be caused by the fast switching of currents in these filters and the most common drawback of APFs is the high cost owing to a large rating inverter. The intermediate way between PPFs and APFs is the use of HAPF that have advantages of PPF and APF.

In [22], the author claims that for a three-phase four-wire non-ideal supply voltage, the conventional synchronous reference frame technique based HAPF fails to give an appreciated response. Therefore, the response of HAPF is improved with the help of a modified PLL that efficiently provides the positive sequence components resulting in a fluently tackling the dynamic behavior methodology. In [23], transformer-less three-phase HAPF design is made that includes few passive components for the upgrading of power quality using PI controller and instantaneous power control.

In [24] fuzzy logic based varying hysteresis band controller is used to reduce the converter switching losses for the HAPF. The LC filter used in [24] cannot effectively tackle the harmonics of the 23rd and 25th order; therefore, an extra block for the extraction of these harmonics from the load current is utilized. However, transformer conversion for low voltage, makes it costly.

In [25], because of controllability and accuracy under periodic disturbance conditions in the power system, a structure-based repetitive control approach with a 31-level cascaded inverter hybrid active filter is presented. This topology increases the complexity and the cost because of the increase in switching devices. Therefore, it is preferred to use the conventional structure and improve the system with controller-based novelty.

In all the aforementioned research work for harmonic analysis, more time is taken by Fast Fourier Transform (FFT) and other topologies involving the correlation function for the extraction of harmonics generated by the nonlinear load. The harmonic elimination with the help of digital filters is not a preferred technique due to its complexity. Moreover, the DFT and FFT methods-based filters are unable to detect the inter harmonics resulting in low efficiency for the reduction of harmonic contamination in power systems. Furthermore, a significant drawback of d-q theory is the inability to detect individual harmonics in a distorted power system. Moreover, the use of a low pass filter affects the response time of the fundamental frequency component.

Therefore, keeping in view the fundamental drawbacks of the aforementioned techniques, in this research, Shunt HAPF is designed for a distorted three phase four wire system with a RNN based novel control algorithm. The HAPF focusses on the elimination of all harmonics, minimization of neutral wire current and switching losses. Therefore, instead of using a four-leg voltage source inverter, a conventional three-leg structure with a split capacitor case is employed with a series connection of PPF and APF and their shunt connection to the system. A comparative analysis of the proposed technique is also presented with conventional techniques, such as p-q theory, PI controller, ANN, and Neuro-Fuzzy Logic. The target is the detection of harmonics in the system and the regulation of the DC voltage.

## III. SYSTEM MODEL

There are different topologies regarding the connection of active and passive components in hybrid APF [26]. To improve the harmonic elimination response of shunt PPF due to nonlinear load, the APF is attached in series with PPF to change the impedance offered by PPF. This method shows a negligible resistance to load side harmonics. The topology

of the SHAPF is illustrated in Figure 2 [26]. In Figure 2, the use of SHAPF reduces the switching losses and voltage rating for the APF due to the low DC link voltage requirement with the prevention of both parallel and series resonance. In real world power systems, the varying operating conditions of the source results in the occurrence of resonance with source current amplification. The relation between harmonic source current and harmonic load current presented in [26], which illustrates the capability of SHAPF to overcome series and parallel resonance. The SHAPF does not have any circulating current problem that occurred in stand-alone PPF and APF. Moreover, if a fault occurs in either PPF or APF, both can easily be bypassed and repaired. Therefore, the advantages of HAPF topology, led us to use this configuration in our paper. The SHAPF behaves as an open circuit for harmonics introduced by nonlinear loads.

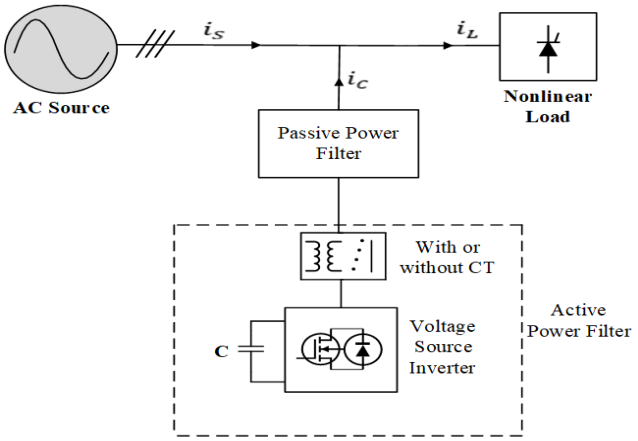


**FIGURE 2.** System with shunt connection of series combination of PPF and APF.

The concept of shunt harmonic current compensation is illustrated in Figure 3 [26]. In Figure 3, the single tuned PPF is used for the elimination of the dominant 5th harmonic because it consumes more reactive power. In Figure 3, the source currents ($i_{sa}, i_{sb}, i_{sc}$) are the sum of load currents ($i_{La}, i_{Lb}, i_{Lc}$) and compensating currents ($i_{ca}, i_{cb}, i_{cc}$). The use of single-phase load is more common in the distribution system therefore, to have a more realistic approach, the nonlinear load comprises of three single-phase rectifiers that are introducing harmonics in the power system. In SHAPF, to avoid harmonic propagation due to resonance of PPF, the harmonic damping can be provided via power line. In Figure 3, the power circuit for the APF consists of center split voltage source inverter made up of six MOSFETs with freewheeling diodes. The midpoint of series DC link capacitors is considered as ground reference **g**, which is connected to the neutral wire. The behavior of the voltage source inverter with hysteresis control pulse width modulation is similar to controlled current source. In Figure 3, the controller of the SHAPF consists of three main functional blocks, such as (a) voltage regulator, (b) reference current calculation, and (c) generation of pulses for inverter switches.

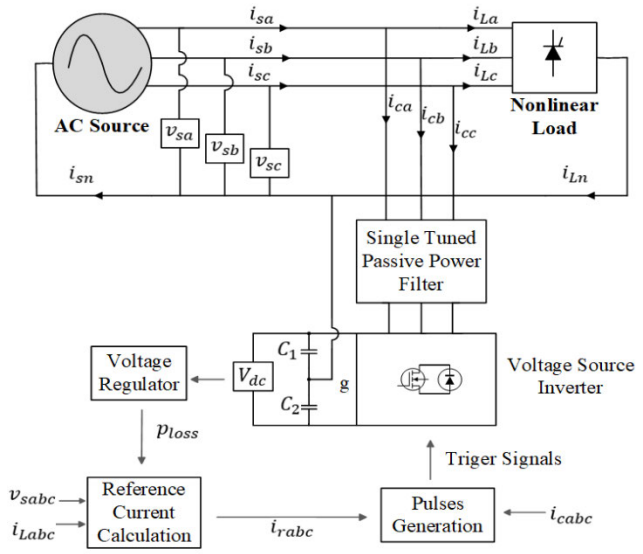


**FIGURE 3.** Shunt harmonic current compensation of the system with nonlinear load [23].

### A. VOLTAGE REGULATOR

The voltage regulator circuit generates a $p_{loss}$ signal from the error signal of voltage reference ($V_{ref}$) and DC link voltage ($V_{dc}$). If $p_{loss}$ signal is not included in the reference current calculation, the DC link capacitor will not charge. For the normal operation of hysteresis control block, the DC link voltage ($V_{dc}$) must be higher than the AC voltage ($V_{L-Lrms}$). The reference DC link voltage for the voltage regulator is computed as [26]:

$$V_{ref} = \frac{2\sqrt{2}V_{L-Lrms}}{\sqrt{3}m}, \tag{1}$$

where the $m$ is the modulation index taken as 1.

### B. REFERENCE CURRENT CALCULATION USING PQ0 THEORY

The instantaneous active and reactive power theory is known as the pq0 theory in a three-phase four-wire system. The pq0 theory-based detailed control activity of SHAPF is depicted in Figure 4 [27]. For the generation of the required harmonic reference currents ($i_{ra}, i_{rb}, i_{rc}$), pq0 theory initiates with the Clarke transformation ($abc$ to $\alpha\beta 0$) for load currents ($i_{La}, i_{Lb}, i_{Lc}$) and source voltages ($v_{sa}, v_{sb}, v_{sc}$). This conversion is used to compute instantaneous powers ($p, q, p_0$) using Eqn. (2) [27].

$$\begin{bmatrix} p \\ q \\ p_0 \end{bmatrix} = \begin{bmatrix} 0 & v_\alpha & v_\beta \\ 0 & v_\beta & -v_\alpha \\ v_0 & 0 & 0 \end{bmatrix} \begin{bmatrix} i_\alpha \\ i_\beta \\ i_0 \end{bmatrix} \tag{2}$$

In pq0 theory, a low pass filter is used to separate average active power ($\bar{p}$) and oscillating active power ($\tilde{p}$) from active power ($p$). A careful selection of the low pass filter is necessary to avoid the compensation errors of harmonics that may occur during transients in the system. In this paper,

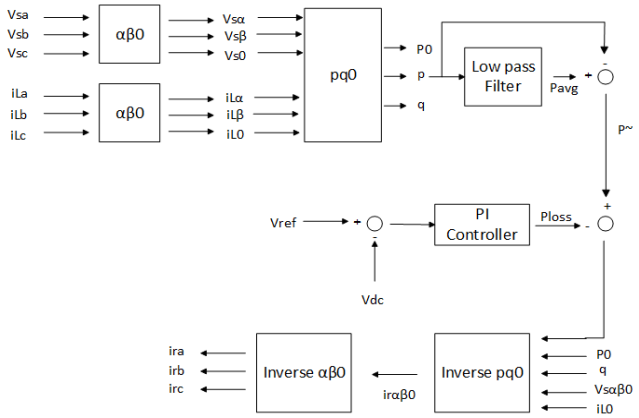


**FIGURE 4.** p-q theory-based harmonic detection in SHAPF [27].

a fourth-order low pass filter is used for the conversion of active power ($p$) into average ($\bar{p}$) and oscillating ($\tilde{p}$) parts.

Voltage regulator determines the excessive part of real power ($p_{loss}$) to maintain the DC voltage ($V_{dc}$) across the split capacitors close to the reference DC link voltage ($V_{ref}$). The active power obtained by the subtraction of $p_{loss}$ from $\tilde{p}$, power due to neutral wire ($p_0$), reactive power ($q$), transformed voltages, and zero sequence load current ($i_{L0}$) are fed to the inverse $pq0$ block. Finally, the reference currents obtained in $\alpha\beta0$ domain from the inverse $pq0$ block using Eqn. (3) and Eqn. (4) are transformed to required $abc$ domain using inverse $\alpha\beta0$ block [27].

$$\begin{bmatrix} i_\alpha \\ i_\beta \\ i_0 \end{bmatrix} = \frac{1}{v_0 A} \begin{bmatrix} v_0 v_\alpha & v_0 v_\beta & 0 \\ v_0 v_\beta & -v_0 v_\alpha & 0 \\ 0 & 0 & A \end{bmatrix} \begin{bmatrix} p \\ q \\ p_0 \end{bmatrix}, \tag{3}$$

where

$$A = v_\alpha^2 + v_\beta^2 \tag{4}$$

### C. HYSTERESIS CONTROL

The hysteresis control method is preferred due to the fast-dynamic response, current limiting capability, and ease of implementation [26]. The reference current ($i_{rabc}$) and filter current ($i_{cabc}$) are compared and their error signal is fed as an input to the hysteresis controller. The output of the controller is a pulse width modulation signal (switching signal) for a three-phase inverter, which generates a similar waveform as the detected harmonic waveform but with phase inversion to eliminate the harmonics in the system.

According to Figure 5, the $+H$ and $-H$ are the upper and lower bounds of the hysteresis band [26]. When the error signal is smaller than $-H$ value, the generated signal will have a high value (1). The hysteresis controller will generate a low value (0) when the error signal is larger than $+H$ value. If the value of error remains between $-H$ and $+H$, then trigger signal will be maintained until the next reverse operation. To avoid short circuit, both switches of the same leg must not be switched on at the same time.

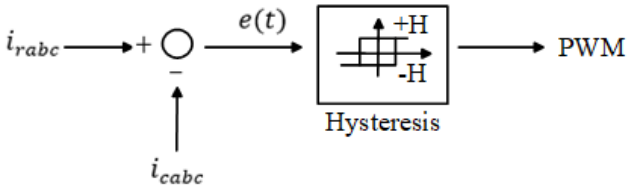


**FIGURE 5.** Hysteresis control for inverter switching [26].

## IV. NEURAL NETWORK BASED PREDICTIVE CONTROL SCHEME

Conventionally, the pq0 theory is employed to compute reference current and PI controller for voltage regulation. However, we are proposing the neural network based predictive control schemes, such as ANN, ANFIS, and RNN architectures to design reference current controller and voltage regulation. The pq0 theory performs better until the supply voltage is in ideal condition [26]. The linear mathematical models of the system are required to design a PI controller, which are difficult to obtain, and may not be suitable to give the desired performance under load variations [28]. Moreover, due to the nonlinear nature of the system, the PI controller does not respond rapidly. The neural networks architectures tend to provide a fast and accurate dynamic response for a nonlinear system containing uncertain information. Therefore, these neural networks are a more suitable options instead of conventional techniques.

### A. ARTIFICIAL NEURAL NETWORK

The ANN algorithm is used to model the complex relationships between the input and output of the system. The feed-forward backpropagation-based ANN control is used in this research work for voltage regulation and harmonic detection. In ANN architecture, hidden layers are used between input and output layers. The ANN has the characteristic to give an improved response by learning from experience and modify itself according to system variations.

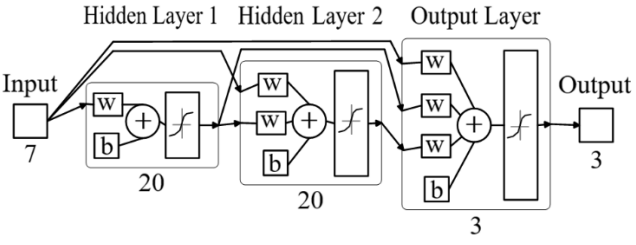


**FIGURE 6.** ANN for harmonic detection in SHAPF [29].

In this paper, for harmonic detection in SHAPF, a similar ANN architecture proposed in [29] is used having a two hidden layer architecture with 20 neurons each, as illustrated in Figure 6. The gradient descent algorithm with momentum is used as the learning function while training the ANN architecture. Levenberg Marquardt's training function is used for the optimization of weights and bias values. Moreover, tan

sigmoid activation function is used in the training of ANN architecture. During the training of ANN, weights and biases are updated iteratively to minimize the error ($e$) between the predicted output ($y_{pred}$). and the required target value ($y_{target}$) as shown in Eqn. (5).

$$e = y_{pred.} - y_{target} \tag{5}$$

In Figure 6, the ANN architecture has seven inputs, three $3-\phi$ source voltages ($v_{sa}, v_{sb}, v_{sc}$), three $3-\phi$ load currents ($i_{La}, i_{Lb}, i_{Lc}$), and the seventh input is the $p_{loss}$ variable obtained from voltage regulation. The harmonic reference currents ($i_{ra}, i_{rb}, i_{rc}$) are the three outputs of the ANN. Similarly, ANN is trained for the voltage regulator with two inputs ($V_{ref}$, and $V_{dc}$) and one output ($p_{loss}$) using two hidden layers each carrying 20 neurons.

### B. RECURRENT NEURAL NETWORK

For sequential data problems, the RNN with Long Short-Term Memory (LSTM) units has emerged as an effective algorithm. The simple RNN structure consists of neural network loops with feedback. The RNN can connect the past information with the present task but there exists a vanishing and exploding gradient problem [30]. During the training, weights of the RNN are updated proportionally to the gradient of error ($e$) with respect to weights ($w_i$). In case of vanishing and exploding gradient problem, gradient becomes very small, thus resulting in the loss of information [31]. In time series problems, RNN faces only vanishing gradient which is accommodated using LSTM units with RNN.

The LSTM units are effective to capture the long-term dependencies temporarily [32]. The structure of the LSTM-based RNN allows time delay connections between the hidden units. This enables the model to maintain the previous information discovering the temporary correlations among the far away events. The ability of memory cells to maintain the data with time and function of information flow gates to allow the flow of required information to or from the memory cell for specific cases is the main idea behind the working principle of LSTM architecture.

This research used LSTM based RNN control models for the regulation of DC voltage and for the detection of harmonics in the SHAPF [30]. In both of the aforementioned controls, LSTM based RNNs are trained using Adam as a training algorithm with 250 epochs and 200 hidden units to make the system more robust and adaptive. The architecture of LSTM based RNN is shown in Figure 7, which includes mathematical computation based three layers in each loop such as:

- The first layer is known as forget gate layer, which uses sigmoid ($\sigma$) for determination of the data that is not required and should be removed from the memory cell. Eqn. (6) represents the working of forget gate layer such as, current input ($X_t$) and output of the previous RNN unit ($H_{t-1}$) modified by respective weights and bias are passed through the sigmoid function resulting in a value between zero and one for the operation of forget gate.

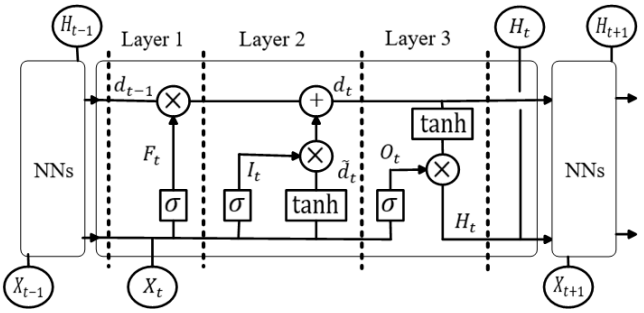


**FIGURE 7.** LSTM architecture for RNN [30].

$$F_t = \sigma\left(w_F\left(H_{t-1}, X_t\right) + b_F\right) \tag{6}$$

- The second layer known as input gate layer, which decides to store new information in memory cell. This layer consists of two steps, such as (a) The values to be updated ($I_t$) are determined by a sigmoid function ($\sigma$) as shown in Eqn. (7), and in Eqn. (8), the *tanh* function is used to find the vector of new candidate values ($\tilde{d}_t$).

$$I_t = \sigma\left(w_I\left(H_{t-1}, X_t\right) + b_I\right) \tag{7}$$

$$\tilde{d}_t = \tanh\left(w_d\left(H_{t-1}, X_t\right) + b_d\right) \tag{8}$$

(b) The old cell state ($F_t \times d_{t-1}$) of the memory cell is updated to the new cell state ($d_t$) using $I_t$ and $\tilde{d}_t$ determined by step (1) as shown in Eqn. (9).

$$d_t = \left(F_t \times d_{t-1}\right) + \left(I_t \times \tilde{d}_t\right) \tag{9}$$

- The third layer is the output gate layer. The sigmoid function here decides the data that should be passed to the next unit of RNN using Eqn. (10). The output ($H_t$) of this layer is generated by passing the memory cell data ($d_t$) through a *tanh* function and multiplying it with the output ($O_t$) of the sigmoid function ($\sigma$) as shown in Eqn. (11).

$$O_t = \sigma\left(w_O\left(H_{t-1}, X_t\right) + b_O\right) \tag{10}$$

$$H_t = O_t \times \tanh\left(d_t\right) \tag{11}$$

### C. ADAPTIVE NEURO-FUZZY INFERENCE SYSTEM

The neuro-fuzzy system based on the approach of Takagi and Sugeno shown in Figure 8 is also known as the Adaptive Neuro-Fuzzy Inference System (ANFIS). The general architecture of the ANFIS algorithm used in the paper consists of five layers and similar to the one used in [33], [34]. The inputs ($X_i$ ) of the system are fed through a linear transfer function to layer 1. Layer 1 is the fuzzification layer corresponding to real values of given inputs. The layer involves determination process to find the membership distribution functions for the inputs. In the result of fuzzification in layer 1, mu ($\mu$) values are obtained. The third layer consists of rules for all possible combinations of input parameters. The $\mu$ values obtained from the first layer are used as inputs in the second layer to compute firing strength ($W$) of this layer. Since the value of $\mu$ lie between 0 to 1; therefore, the value of $W$ will be in

the range of 0 to 1. In layer 3, the normalized value of $W$ is determined for each neuron, such as the normalized value for the first neuron ($\overline{W_1}$) is obtained using Eqn. (12) [33], [34]. The output in layer 4 is obtained by multiplication of the results of the previous two layers. To generate the final output, products of layer 4 are added together in the fifth layer, which is also known as the defuzzification layer.

$$\overline{W_1} = \frac{W_1}{W_1 + W_2 + W_3 + \ldots + W_i} \tag{12}$$

In layer 1 and layer 5, the selection of optimization algorithm for ANFIS tuning can improve the model performance. In the paper, the backpropagation optimization algorithm is used for the training of ANFIS. Moreover, the performance of ANFIS also depends on the appropriate selection of membership function distribution for the input variables. Therefore, the selection of linear membership functions, such as triangular membership function [28] is an easy approach but it is unable to give a precise response [33], [34]. To achieve more accuracy, we select a nonlinear membership function, such as the Gauss membership function. The gaussian distribution is a bell-shaped function (low, and high values) having some overlapping regions.

To design the controller for voltage regulator in SHAPF, there is a single input ($e(t)$) and single output ($p_{loss}$). We select 17 membership functions for the input $e(t)$ and the output is selected as linear. Therefore, the ANFIS structure used in the paper has 17 rules.

For the detection of harmonics, three multi-input and single output ANFIS models are constructed for each phase reference current generation. Two membership functions are taken for each of the input to generate the reference harmonic currents ($i_{ra}$, $i_{rb}$, $i_{rc}$). Since there are seven inputs for harmonic detection; therefore, each ANFIS model in this control block has 49 rules.

## V. RESULTS AND DISCUSSIONS

The proposed neural network-based controllers for hybrid SHAPF presented in Figure 3 are evaluated and compared with respect to power quality maintenance of the power system under study. A series of simulations are performed, and response of proposed control techniques based SHAPF are presented in this Section. It is worth mentioning that the selection for the number of neurons for all three architectures are considered suitable based on 50 trail runs each. Moreover, a comparison of proposed techniques is made with the existing conventional technique, such as the pq0 theory with the PI controller. The applicability of designed control techniques is characterized by three cases employing different nonlinear load scenarios are described in Table 1, having a balanced supply voltage. Moreover, power system specifications to validate the simulations of SHAPF for the aforementioned three load cases are presented in Table 2.

For a balanced sinusoidal supply with a directly connected nonlinear load, the designed SHAPF targets to filter the harmonic contaminated source current only. For Test

**TABLE 1. Test cases considered for the proposed work.**

| Test Cases | pq0 with PI | ANN | ANFIS | RNN |
|---|---|---|---|---|
| ***Case 1*** (3-phase rectifier with fixed RLC load) | ✓ | ✓ | ✓ | ✓ |
| ***Case 2*** (3-phase rectifier with variable RLC load) | ✓ | ✓ | ✓ | ✓ |
| ***Case 3*** (3-phase rectifier with fixed RLC load and DC Motor) | ✓ | ✓ | ✓ | ✓ |

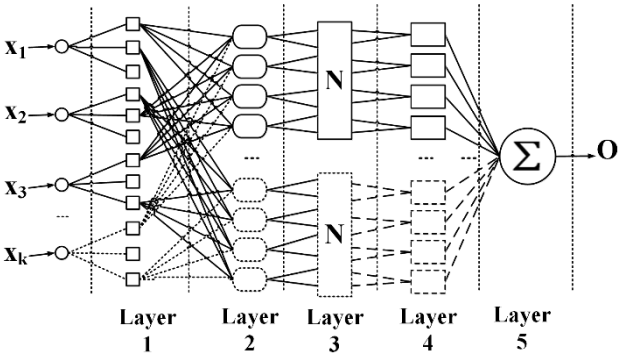


**FIGURE 8. General architecture of ANFIS.**

**TABLE 2. Parameters for testing the system response with designed SHAPF.**

| System parameters | Physical values |
|---|---|
| Phase voltage rms value | 220 V |
| Frequency | 50 Hz |
| $R_f$ | 1 $m\Omega$ |
| $L_f$ | 3 $m$H |
| $C_1 = C_2$ | 470 $\mu F$ |
| $V_{ref}$ | 622 V DC |
| $k_p$ | 25 |
| $k_i$ | 17 |
| Power rating | 10 KVA |
| 3 Single phase rectifiers and DC motor based nonlinear load (R, L, and C) | 43.2 Ω , 34.5 $m$H, 292 $\mu F$ (720 VAR) |

Case 1, without SHAPF, the power system has three-phase distorted current with 58.70% THD in phase a, 67.42% THD in phase b, and 50.82% THD in phase c. The conventional pq0 theory with PI controller based SHAPF reduces the harmonic contamination to 3.08% THD in phase a, 5.03% THD in phase b, and 3.79% THD in phase c. Moreover, the compensation current is produced by the SHAPF because of the harmonics detected in the system. The neutral wire originally caries 12A current because of the disturbance in the system introduced by the nonlinear load. The SHAPF

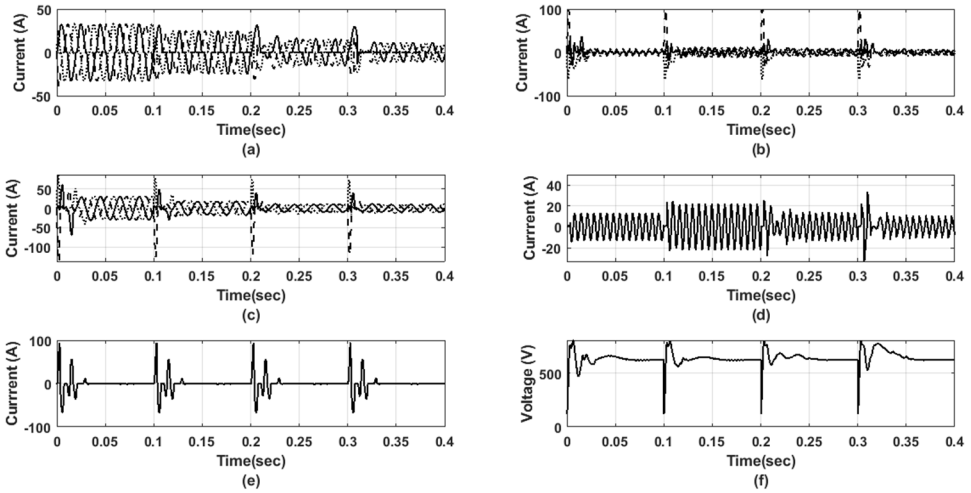


**FIGURE 9.** Analysis of case 2 using pq0 theory and the PI controller technique: (a) load current, (b) filter current, (c) source current, (d) neutral wire current on load side, (e) neutral wire current on source side, (f) DC voltage regulation.

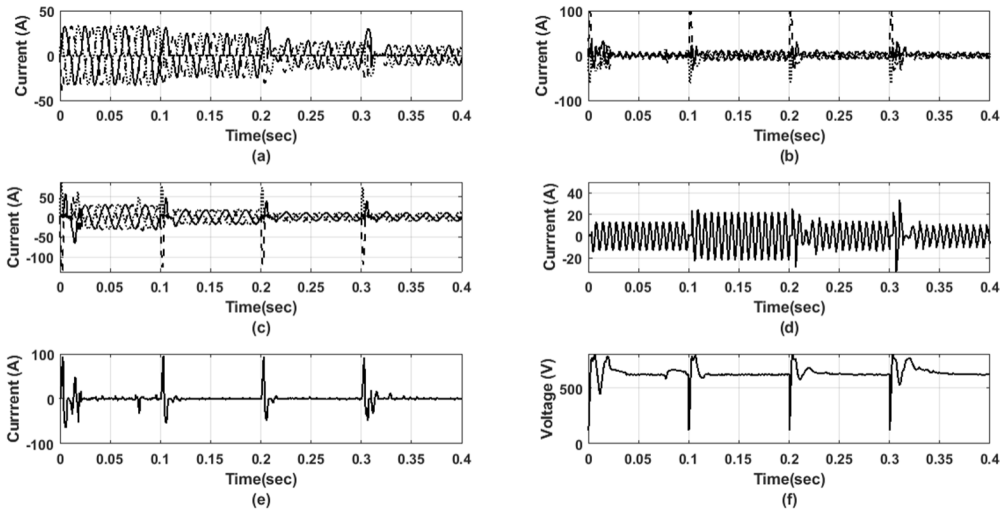


**FIGURE 10.** Analysis of case 2 using ANN technique: (a) load current, (b) filter current, (c) source current, (d) neutral wire current on load side, (e) neutral wire current on source side, (f) DC voltage regulation.

minimizes the neutral wire current on the source side to 0.90A with the conventional pq0 theory with PI controller. The PI controller regulates the DC voltage according to the required set point with the response time of 0.06 seconds. The reduction of harmonic distortion in the system depends on the efficiency of control technique to detect the tendency of harmonics present in the system, and the generation of the compensation current accordingly.

Similarly, the behavior of the power system for test Case 1 using ANN, ANFIS, and RNN techniques based SHAPF simulations are also observed. The THD of source current is reduced to 3.29% in phase a, 4.20% in phase b, and 3.73% in phase c using ANN control technique. ANFIS based control topology reduces the source current THD to 3.35% in phase a, 3.99% in phase b, and 3.30% in phase c. The RNN based controller minimizes the THD to 2.94% in phase a, 5.01% in phase b, and 2.97% in phase c. Moreover, the designed SHAPF also improved the power factor of the system. The RNN technique based SHAPF gives the lowest neutral wire current of 0.45A with minimum DC voltage fluctuations as compared to the ANN, ANFIS, and conventional pq0 theory with PI controller.

The analysis of system response in test Case 2 with the conventional technique is illustrated in Figure 9. The load current, filter current, source current, neutral wire current on the load side, neutral wire current on source side, and the DC voltage regulation are presented in Figure 9 subplots (a), (b), (c), (d), (e), and (f), respectively. In test Case 2, the three-phases are connected separately with three single-phase rectifiers along with a reference RLC taken as same in test Case 1. However, the RLC load is varied in three sub-cases, such as (a) 25% of RLC load, (b) 50% of RLC

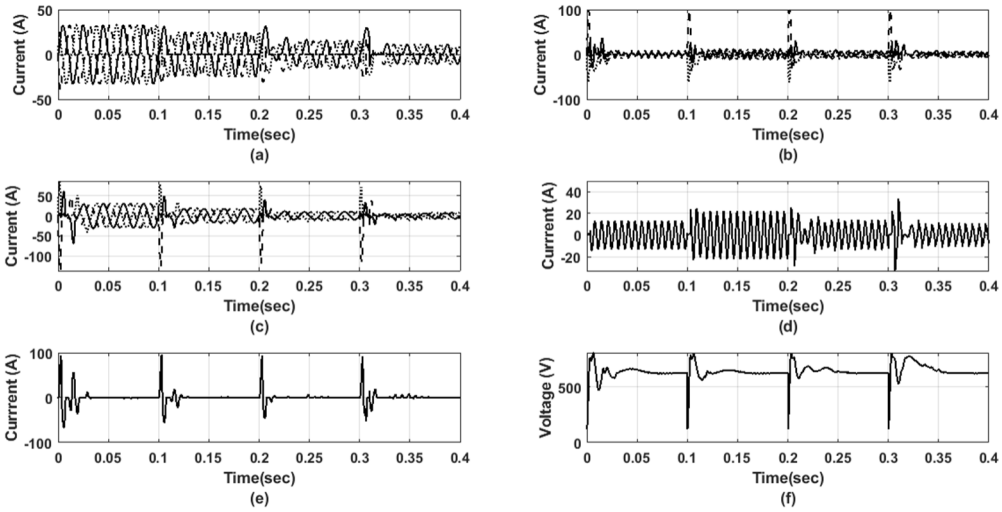


**FIGURE 11.** Analysis of case 2 using Adaptive Neuro Fuzzy Inference System technique: (a) load current, (b) filter current, (c) source current, (d) neutral wire current on load side, (e) neutral wire current on source side, (f) DC voltage regulation.

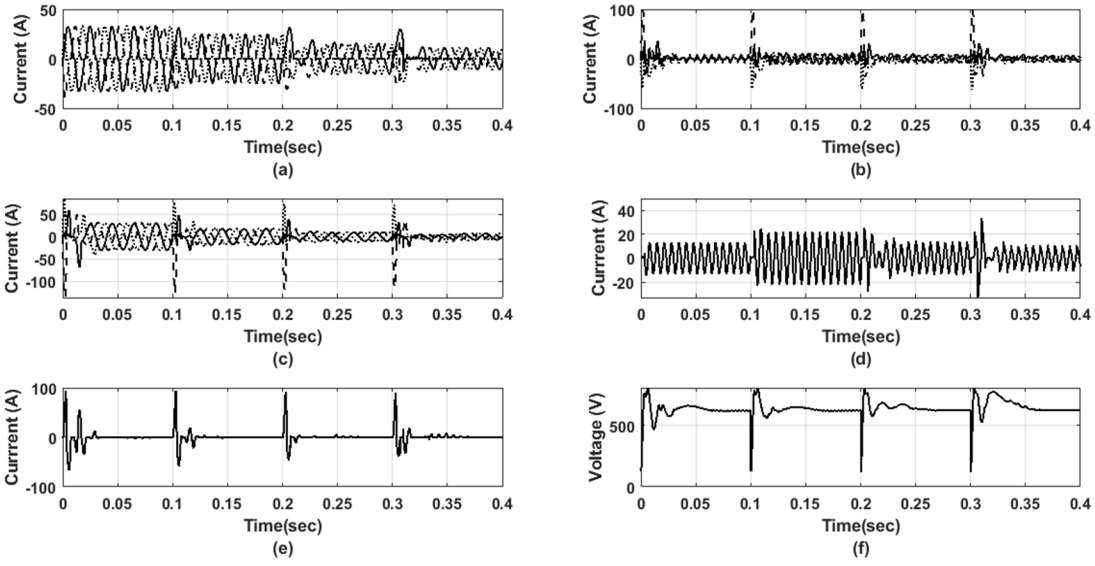


**FIGURE 12.** Analysis of case 2 using Recurrent Neural Network technique: (a) load current, (b) filter current, (c) source current, (d) neutral wire current on load side, (e) neutral wire current on source side, (f) DC voltage regulation.

load, (c) 75% of RLC load, (d) 100% of RLC load. The amplitude of current and the extent of distortions in the system varies according to the connected load variation. Originally, the system with 25% RLC load contains a 15.27% THD in phase a, 17.89% THD in phase b, and 17.59% THD in phase c. The conventional pq0 theory with PI controller reduces the THD in phase a to 3.62%, 7.22% in phase b, and 2.35% in phase c. The neutral wire current on the sources side was equal to the neural wire current on the load side and the average value of the current was 12.952A, as shown in Figure 9(d). The conventional pq0 theory with PI controller based reduce the neural wire current on the source side to 0.179A, as shown in Figure 9(e). When the nonlinear load changes to 50% of the RLC load, the three-phases originally contain 37.29%, 38.37%, and 37.98% THDs, respectively. The harmonic contamination is reduced in the aforementioned load condition to 2.49%, 3.16% in phase b, and 4.00% in phase c with minimization of neutral wire current from 22.149A to 0.179A. Varying the nonlinear load to 75% RLC load introduces 42.10% THD in phase a, 44.57% THD in phase b, and 41.59% THD in phase c without SHAPF. The use of conventional pq0 theory with PI controller based SHAPF minimize the THDs to 5.06%, 6.44%, and 5.09% in phase a, b, and c, respectively. For sub-case four with 100% RLC load, the increase in THDs for the three-phases is also satisfactorily mitigated according to the international standards with the elimination of neutral wire current, as illustrated in Table 3.

**TABLE 3. Comparison of total harmonic distortion (THD).**

| | | Source Current THD (%) | | | Load Current THD (%) | | | Power Factor with filter | | | Power Factor without filter | | |
|---|---|---|---|---|---|---|---|---|---|---|---|---|---|
| Case No. | Method | Phase A | Phase B | Phase C | Phase A | Phase B | Phase C | Phase A | Phase B | Phase C | Phase A | Phase B | Phase C |
| Case 1 | pq0 with PI | 3.08 | 5.03 | 3.79 | 58.70 | 67.42 | 50.82 | 1 | 0.9999 | 1 | 0.8309 | 0.7886 | 0.8036 |
| | ANN | 3.29 | 4.20 | 3.73 | 58.70 | 67.42 | 50.82 | 1 | 1 | 1 | | | |
| | ANFIS | 3.35 | 3.99 | 3.30 | 58.70 | 67.42 | 50.82 | 0.9998 | 0.9997 | 1 | | | |
| | RNN | 2.94 | 5.01 | 2.97 | 58.70 | 67.42 | 50.82 | 1 | 1 | 1 | | | |
| Case 2 (a) | pq0 with PI | 3.62 | 7.22 | 2.35 | 15.27 | 17.89 | 17.59 | 1 | 1 | 1 | 0.9999 | 0.9978 | 0.9968 |
| | ANN | 6.29 | 5.98 | 12.30 | 15.27 | 17.89 | 17.59 | 0.9999 | 0.9999 | 1 | | | |
| | ANFIS | 3.60 | 3.23 | 5.36 | 15.27 | 17.89 | 17.59 | 1 | 1 | 1 | | | |
| | RNN | 1.90 | 2.07 | 2.12 | 15.27 | 17.89 | 17.59 | 1 | 1 | 1 | | | |
| Case 2 (b) | pq0 with PI | 2.49 | 2.30 | 2.56 | 37.29 | 38.37 | 37.98 | 1 | 1 | 1 | 0.9603 | 0.9176 | 0.9156 |
| | ANN | 3.25 | 3.16 | 4.00 | 37.29 | 38.37 | 37.98 | 0.9683 | 0.9385 | 0.9879 | | | |
| | ANFIS | 2.49 | 2.02 | 2.05 | 37.29 | 38.37 | 37.98 | 1 | 1 | 1 | | | |
| | RNN | 2.05 | 2.00 | 1.90 | 37.29 | 38.37 | 37.97 | 1 | 1 | 1 | | | |
| Case 2 (c) | pq0 with PI | 5.06 | 6.44 | 5.09 | 42.10 | 44.57 | 41.59 | 1 | 1 | 1 | 0.8626 | 0.8139 | 0.8259 |
| | ANN | 6.36 | 10.29 | 9.23 | 42.10 | 44.57 | 41.59 | 0.9939 | 0.9984 | 0.9709 | | | |
| | ANFIS | 5.55 | 6.43 | 5.06 | 42.10 | 44.57 | 41.59 | | | | | | |
| | RNN | 2.30 | 4.22 | 5.01 | 42.10 | 44.52 | 41.57 | 1 | 1 | 1 | | | |
| Case 2 (d) | pq0 with PI | 3.55 | 8.18 | 5.35 | 58.70 | 67.42 | 50.82 | 1 | 1 | 1 | 0.8319 | 0.7887 | 0.8035 |
| | ANN | 8.96 | 9.69 | 9.54 | 58.70 | 67.42 | 50.82 | 1 | 0.9995 | 1 | | | |
| | ANFIS | 3.37 | 5.01 | 3.97 | 58.70 | 67.42 | 50.82 | | | | | | |
| | RNN | 3.36 | 4.87 | 3.35 | 58.70 | 67.42 | 50.82 | 1 | 1 | 1 | | | |
| Case 3 | pq0 with PI | 3.17 | 4.01 | 3.45 | 57.04 | 61.17 | 48.13 | 1 | 1 | 1 | 0.8264 | 0.7853 | 0.8009 |
| | ANN | 3.16 | 4.91 | 3.35 | 57.04 | 61.17 | 48.13 | 1 | 1 | 1 | | | |
| | ANFIS | 3.30 | 7.62 | 4.16 | 57.04 | 61.17 | 48.13 | | | | | | |
| | RNN | 2.79 | 3.35 | 3.01 | 57.04 | 61.17 | 48.13 | 1 | 1 | 1 | | | |

The analysis of test Case 2 using neural network-based techniques, such as ANN, ANFIS, and RNN are presented in Figure 10, Figure 11, and Figure 12, respectively. In Figure 10(f), the voltage regulator becomes stable at 0.035sec. for 25% RLC load scenario but the regulator fails the stability condition at 0.85sec. and the impact is observed in the form of low minimization of THD and neutral wire current. The aforementioned condition does not occur when the load values go beyond 25% RLC load scenario. The overall response of the ANN-based controller trained for the variable load condition is not satisfactory as compared to the conventional pq0 theory with PI controller-based technique. Employing the ANN control technique, the harmonic distortion obtained for test Case 2 still satisfy the international standards.

In the four different load variations of test Case 2, the proposed RNN based SHAPF technique is the most proficient and robust. The RNN based controller for SHAPF gives minimum THD and neutral wire current for the system under consideration compared to all other applied techniques. The comprehensive comparative analysis results are presented in Table 3. All the techniques used are compared based on source current THD, load current THD, and power factor improvement. Moreover, the comparative analysis of neutral wire current and DC voltage fluctuations in the regulator is presented in Table 4. It is evident from comparative analysis that the RNN based controller clearly outperforms other employed techniques.

The comparative analysis of test Case 3 comprising of three single-phase rectifiers and DC motor nonlinear load is also depicted in Table 3 and Table 4. Similarly, the RNN based controller for SHAPF is comparatively better in test Case 3. In this scenario, the system has the lowest 2.79% THD for phase a, 3.35% THD for phase b, and 3.01% THD for phase c. The neutral wire was originally carrying a current of 9.758A, reduced to the minimum level of 0.414A compared to other techniques. The DC voltage fluctuations are not minimum with RNN for test Case 3; however, the voltage fluctuations are still within the required range to give minimum THD. The power factor of the system source side is measured after the mitigation of distortions using Eqn. (13), i.e.,

$$\cos\theta = \frac{P}{S}. \tag{13}$$

In Eqn. (13), $P$ is the real power, and $S$ is the apparent power. The angle $\theta$ is measured between the zero crossings of sinusoidal voltage and the current waveform.

In Addition, we conducted a thorough comparison for the elimination of series and parallel resonance in the system. To show the effectiveness of the proposed SHAPF and its

**TABLE 4.** Comparison of neutral wire current and DC voltage fluctuations.

| Cases | Methods | Neutral Wire Current (A) | DC Voltage Fluctuations (V) |
|---|---|---|---|
| Case 1 | pq0 with PI | 0.900 | 3.8912 |
| | ANN | 0.650 | 1.7948 |
| | ANFIS | 5.550 | 5.2129 |
| | RNN | 0.450 | 1.6748 |
| Case 2(a) | pq0 with PI | 0.179 | 8.1481 |
| | ANN | 2.723 | 9.5267 |
| | ANFIS | 0.170 | 6.1491 |
| | RNN | 0.177 | 5.4005 |
| Case 2(b) | pq0 with PI | 1.441 | 6.1872 |
| | ANN | 2.230 | 8.4027 |
| | ANFIS | 0.175 | 4.9359 |
| | RNN | 0.108 | 3.1365 |
| Case 2(c) | pq0 with PI | 0.527 | 3.4344 |
| | ANN | 2.274 | 9.622 |
| | ANFIS | 0.183 | 3.3839 |
| | RNN | 0.610 | 2.712 |
| Case 2(d) | pq0 with PI | 0.900 | 3.8912 |
| | ANN | 0.650 | 1.7948 |
| | ANFIS | 5.550 | 5.2129 |
| | RNN | 0.450 | 1.6748 |
| Case 3 | pq0 with PI | 0.567 | 3.6273 |
| | ANN | 0.512 | 1.7099 |
| | ANFIS | 0.414 | 2.8776 |
| | RNN | 0.354 | 3.2873 |

**TABLE 5.** Simulation results before Compensation and after PPF and SHAPF compensation separately.

| Capabilities | Method | Before compensation | | | After compensation | | |
|---|---|---|---|---|---|---|---|
| | | $THD_{IS}$ (%) | $I_{Sn}$ (A) | DPF | $THD_{IS}$ (%) | $I_{Sn}$ (A) | DPF |
| Parallel Resonance Prevention | PPF | 35.84 | 12.0 | 0.78 | 40.00 | 10.42 | 0.97 |
| | SHAPF | 35.84 | 12.0 | 0.78 | 3.17 | 0.570 | 0.99 |
| Series Resonance Prevention | PPF | 35.84 | 12.0 | 0.78 | 51.09 | 13.90 | 0.98 |
| | SHAPF | 35.84 | 12.0 | 0.78 | 4.38 | 0.610 | 1.00 |

comparison with PPF, Table 5 presents the detailed analysis of system response before applying the compensation circuit and after applying PPF and SHAPF separately. Moreover, the results shown in Table 5 are representing the resonance condition for test Case 3 as it is the most complex case considered in our study. The comparison is conducted based on THD of system current ($i_S$), system's neutral current ($I_{Sn}$), and system's displacement power factor (DPF). This verifies the capability of SHAPF to eliminate the effect of series and parallel resonance due to variations in source operating conditions. Moreover, we can observe from Table 5 that by using only PPF, the THD of system current is increased to 40% in case of parallel resonance and 51.09% in case of series resonance because PPF is unable to suppress the 3$^{rd}$ harmonic per resonance, while SHAPF is working effectively as the THD of system current and $I_{Sn}$ are reduced significantly, while DPF also improved.

## VI. CONCLUSION AND FUTURE WORK

In this paper, a comparative analysis of conventional pq0 theory with PI controller and neural network-based control procedures for the SHAPF is presented to improve the power quality of the non-sinusoidal power system. The structure of the proposed three-phase filter is designed to eliminate the harmonics and neutral wire current. The RNN based control strategy for the extraction of harmonics present in the system and the DC voltage regulation is encouraging approach due to robustness and more capability for filtering. The dependency of the proposed technique is analyzed and compared using three different case scenarios. The simulated response reviled the significance such as: (a) In the three different case scenarios, the proposed techniques were used for the compensating current infusion and the DC voltage regulation, (b) The THD and neutral wire current are diminished to the minimum level by using the RNN control technique, and (c) All the techniques applied in the paper eliminate the current harmonics according to the desired range of the IEEE and IET standards with the improvement in power factor. In future work, the proposed filter will be extended by Hardware-in-Loop implementation and implementation in a local textile industry, which is the second phase of our approved funded project. Moreover, complex hybrid control technique will be applied to further improve the response of the SHAPF. Finally, we intend further experimenting with both deep and statistical machine learning models as in [35] and [36].

## DATA AVAILABILITY

*Simulations and Related Data to this article can be found at* DOI: http://dx.doi.org/10.17632/ywrdf462dz.1#file-cbbc68f9-25fd-4f13-b15f-5796d2523130, *an open-source online data repository hosted at Mendeley Data (Jawad and Iqbal, 2020).*

## REFERENCES

[1] E. Gunther, "Harmonic and interharmonic measurement according to IEEE 519 and IEC 61000-4-7," in *Proc. IEEE/PES Transmiss. Distrib. Conf. Exhib.*, Dallas, TX, USA, May 2006 pp. 223–225.

[2] J. C. Das, *Power System Harmonics and Passive Filter Designs*. Piscataway, NJ, USA: Institute of Electrical and Electronics Engineers, Mar. 2015.

[3] H. Kazem, "Harmonic mitigation techniques applied to power distribution networks," *Adv. Power Electron.*, vo1. 2013, Feb. 2013, Art. no. 591680.

[4] M. R. Jannesar, A. Sedighi, M. Savaghebi, A. Anvari-Moghaddam, and J. M. Guerrero, "Optimal probabilistic planning of passive harmonic filters in distribution networks with high penetration of photovoltaic generation," *Int. J. Electr. Power Energy Syst.*, vol. 110, pp. 332–348, Sep. 2019.

[5] W. Yeetum and V. Kinnares, "Parallel active power filter based on source current detection for antiparallel resonance with robustness to parameter variations in power systems," *IEEE Trans. Ind. Electron.*, vol. 66, no. 2, pp. 876–886, Feb. 2019.

[6] M. Omran, I. Ibrahim, A. Ahmad, M. Salem, M. Almelian, A. Jusoh, and T. Sutikno, "Comparisons of PI and ANN controllers for shunt HPF based on STF-PQ algorithm under distorted grid voltage," *Int. J. Power Electron. Drive Syst.*, vol. 10, no. 3, pp. 1339–1346, 2019.

[7] D. O. Abdeslam, P. Wira, J. Merckle, D. Flieller, and Y.-A. Chapuis, "A unified artificial neural network architecture for active power filters," *IEEE Trans. Ind. Electron.*, vol. 54, no. 1, pp. 61–76, Feb. 2007.

[8] E. Kazemi-Robati and M. S. Sepasian, "Passive harmonic filter planning considering daily load variations and distribution system reconfiguration," *Electr. Power Syst. Res.*, vol. 166, pp. 125–135, Jan. 2019.

[9] M. M. Elkholy, M. A. El-Hameed, and A. A. El-Fergany, "Harmonic analysis of hybrid renewable microgrids comprising optimal design of passive filters and uncertainties," *Electr. Power Syst. Res.*, vol. 163, pp. 491–501, Oct. 2018.

[10] E. L. L. Fabricio, S. C. S. Junior, C. B. Jacobina, and M. B. de Rossiter Correa, "Analysis of main topologies of shunt active power filters applied to four-wire systems," *IEEE Trans. Power Electron.*, vol. 33, no. 3, pp. 2100–2112, Mar. 2018.

[11] P. Santiprapan, K. L. Areerak, and K. N. Areerak, "Mathematical model and control strategy on DQ frame for shunt active power filters," *Int. J. Electr., Comput., Energetic, Electron. Commun. Eng.*, vol. 5, no. 12, pp. 1–9, 2011.

[12] H. C. Lin, "Intelligent neural network-based fast power system harmonic detection," *IEEE Trans. Ind. Electron.*, vol. 54, no. 1, pp. 43–52, Feb. 2007.

[13] K. Nishida, M. Rukonuzzaman, and M. Nakaoka, "A novel single-phase shunt active power filter with adaptive neural network based harmonic detection," *IEEJ Trans. Ind. Appl.*, vol. 125, no. 1, pp. 9–15, 2005.

[14] J. Fei and Y. Chu, "Double hidden layer output feedback neural adaptive global sliding mode control of active power filter," *IEEE Trans. Power Electron.*, vol. 35, no. 3, pp. 3069–3084, Mar. 2020.

[15] M. Qasim, P. Kanjiya, and V. Khadkikar, "Artificial-neural-network-based phase-locking scheme for active power filters," *IEEE Trans. Ind. Electron.*, vol. 61, no. 8, pp. 3857–3866, Aug. 2014.

[16] L. Hamiche, S. Saad, L. Merabet, and F. Zaamouche, "Adaline neural network and real-imaginary instantaneous powers method for harmonic identification," *Synthèse, Revue des Sci. et de la Technologie*, vol. 36, no. 1, pp. 129–140, Jun. 2018.

[17] R. Guzman, L. G. de Vicuña, J. Morales, M. Castilla, and J. Miret, "Model-based control for a three-phase shunt active power filter," *IEEE Trans. Ind. Electron.*, vol. 63, no. 7, pp. 3998–4007, Jul. 2016.

[18] R. Chilipi, N. Al Sayari, K. Al Hosani, M. Fasil, and A. R. Beig, "Third order sinusoidal integrator (TOSSI)-based control algorithm for shunt active power filter under distorted and unbalanced voltage conditions," *Int. J. Electr. Power Energy Syst.*, vol. 96, pp. 152–162, Mar. 2018.

[19] H. Bellatreche, M. Bounekhla, and A. Tlemcani, "Using fuzzy logic and hysteresis current control to reduce harmonics in three level NPC shunt active power filter," in *Proc. 8th Int. Conf. Modeling, Identificat. Control (ICMIC)*, Algiers, Algeria, Nov. 2016, pp. 5–9.

[20] A. A. A. Elgammal and M. F. El-Naggar, "MOPSO-based optimal control of shunt active power filter using a variable structure fuzzy logic sliding mode controller for hybrid (FC-PV-wind-battery) energy utilisation scheme," *IET Renew. Power Gener.*, vol. 11, no. 8, pp. 1148–1156, Jun. 2017.

[21] W.-H. Ko and J.-C. Gu, "Impact of shunt active harmonic filter on harmonic current distortion of voltage source inverter-fed drives," *IEEE Trans. Ind. Appl.*, vol. 52, no. 4, pp. 2816–2825, Jul. 2016.

[22] P. Dey and S. Mekhilef, "Current harmonics compensation with three-phase four-wire shunt hybrid active power filter based on modified D–Q theory," *IET Power Electron.*, vol. 8, no. 11, pp. 2265–2280, Nov. 2015.

[23] M. N. Rashmi, A. Meenakshi, M. Namratha, S. V. Nayana, and K. Archana, "Power quality improvement using hybrid filters," in *Proc. 3rd IEEE Int. Conf. Recent Trends Electron., Inf. Commun. Technol. (RTEICT)*, Bangalore, India, May 2018, pp. 804–808.

[24] E. Durna, "Adaptive fuzzy hysteresis band current control for reducing switching losses of hybrid active power filter," *IET Power Electron.*, vol. 11, no. 5, pp. 937–944, May 2018.

[25] B. Sahoo, S. K. Routray, and P. K. Rout, "Repetitive control and cascaded multilevel inverter with integrated hybrid active filter capability for wind energy conversion system," *Eng. Sci. Technol., Int. J.*, vol. 22, no. 3, pp. 811–826, Jun. 2019.

[26] C. Lam and M. Wong, *Design and Control of Hybrid Active Power Filters*. Berlin, Germany: Springer-Verlag, 2014, pp. 23–37.

[27] H. Akagi, E. H. Watanabe, and M. Aredes, *Instantaneous Power Theory and Applications to Power Conditioning*, 2nd ed. Piscataway, NJ, USA: IEEE Press, 2017.

[28] S. Mikkili and A. K. Panda, "Instantaneous active and reactive power and current strategies for current harmonics cancellation in 3-ph 4wire SHAF with both PI and fuzzy controllers," *Energy Power Eng.*, vol. 3, no. 3, pp. 285–298, 2011.

[29] M. Jawad, M. Qureshi, M. U. S. Khan, S. Ali, X. Wang, A. Mehmood, B. Khan, and S. U. Khan, "A robust optimization technique for energy cost minimization of cloud data centers," *IEEE Trans. Cloud Comput.*, early access, Nov. 7, 2018, doi: 10.1109/TCC.2018.2879948.

[30] N. Shabbir, L. Kutt, M. Jawad, R. Amadiahanger, M. N. Iqbal, and A. Rosin, "Wind energy forecasting using recurrent neural networks," in *Proc. Big Data, Knowl. Control Syst. Eng. (BdKCSE)*, Sofia, Bulgaria, Nov. 2019, pp. 1–5.

[31] M. A. Nielsen, *Neural Networks and Deep Learning*. San Francisco, CA, USA: Determination Press, 2015.

[32] K. Greff, R. K. Srivastava, J. Koutník, B. R. Steunebrink, and J. Schmidhuber, "LSTM: A search space odyssey," *IEEE Trans. Neural Netw. Learn. Syst.*, vol. 28, no. 10, pp. 2222–2232, Oct. 2017.

[33] S. Ayyaz, U. Qamar, and R. Nawaz, "HCF-CRS: A hybrid content based fuzzy conformal recommender system for providing recommendations with confidence," *PLoS ONE*, vol. 13, no. 10, Oct. 2018, Art. no. e0204849.

[34] S. Ali, F. Mehmood, D. Dancey, Y. Ayaz, M. J. Khan, N. Naseer, R. D. C. Amadeu, H. Sadia, and R. Nawaz, "An adaptive multi-robot therapy for improving joint attention and imitation of ASD children," *IEEE Access*, vol. 7, pp. 81808–81825, 2019.

[35] R. Yunus, O. Arif, H. Afzal, M. F. Amjad, H. Abbas, H. N. Bokhari, S. T. Haider, N. Zafar, and R. Nawaz, "A framework to estimate the nutritional value of food in real time using deep learning techniques," *IEEE Access*, vol. 7, pp. 2643–2652, 2019.

[36] S.-U. Hassan, M. Imran, S. Iqbal, N. R. Aljohani, and R. Nawaz, "Deep context of citations using machine-learning models in scholarly full-text articles," *Scientometrics*, vol. 117, no. 3, pp. 1645–1662, Oct. 2018.